Adsorption and Aggregation of Cationic Amphiphilic Polyelectrolytes on Silica

ARTICLE *in* LANGMUIR · APRIL 2005

Impact Factor: 4.46 · DOI: 10.1021/la047311y · Source: PubMed

6 AUTHORS, INCLUDING:

Karin Schillén
Lund University
80 PUBLICATIONS **2,867** CITATIONS
SEE PROFILE

Bjorn Lindman
Lund University
575 PUBLICATIONS **19,821** CITATIONS
SEE PROFILE

Adsorption and Aggregation of Cationic Amphiphilic Polyelectrolytes on Silica

Yulia Samoshina,[†] Tommy Nylander,*[,†] Per Claesson,[‡] Karin Schillén,[†] Ilias Iliopoulos,[§] and Björn Lindman[†]

Physical Chemistry 1, Lund University, P. O. Box 124, SE-22100 Lund, Sweden, Department of Chemistry, Surface Chemistry, Royal Institute of Technology, SE-10044, Stockholm, Sweden, Institute for Surface Chemistry, P. O. Box 5607, SE-11486 Stockholm, Sweden, and Matière Molle et Chimie, UMR-7167, ESPCI-CNRS, 10 Rue Vauquelin, F-75231 Paris Cedex 05, France

Received November 2, 2004. In Final Form: December 22, 2004

The adsorption of two cationic amphiphilic polyelectrolytes, which are copolymers of two charged monomers, triethyl(vinylbenzyl)ammonium chloride and dimethyldodecyl(vinylbenzyl)ammonium chloride (which is the amphiphilic one) with different contents of amphiphilic groups (40% (40DT) and 80% (80DT)), onto the hydrophilic silica−aqueous solution interface has been studied by in situ null ellipsometry and tapping mode atomic force microscopy (AFM). Adsorption isotherms for both polyelectrolytes were obtained at 25 °C and at different ionic strengths, and the adsorption kinetics was also investigated. At low ionic strength, thin adsorbed layers were observed for both polyelectrolytes. The adsorption increases with polymer concentration and reaches, in most cases, a plateau at a concentration below 50 ppm. For the 80DT polymer, at higher ionic strength, an association into aggregates occurs at concentrations at and above 50 ppm. The aggregates were observed directly by AFM at the surface, and by dynamic light scattering in the solution. The adsorption data for this case demonstrated multilayer formation, which correlates well with the increase in viscosity with the ionic strength observed for 80DT.

1. Introduction

Hydrophobically modified polyelectrolytes (HMPEs) can be divided into three main classes: block copolymers, associating polyelectrolytes and polymeric surfactants (including copolymers with different densities of amphiphilic segments), or polysoaps.[1] They are used in many industrial applications to modify surface properties as the adsorption behavior can be adjusted both by chemical modification and by manipulating the ionic strength of the solution. The HMPEs are therefore currently used in several industrial products such as paints, cosmetics, and pharmaceutical formulations in order to control the rheology and stability of complex fluids.[2−5] One example is the stabilization of aqueous dispersions of hydrophobic colloids.[2] These types of polymers have also come into use for building core−shell morphologies at surfaces with potential use in drug delivery systems.[6] Polymeric surfactants (with different densities of the amphiphilic segments) dissolved in aqueous solutions are known to adopt micelle-like microphase structures, where hydrophobic substitutes form the interior domains and charged segments form outer layers. These structures are often referred to as unimolecular micelles. For large enough polymers one polymer molecule can contain several unimolecular micelles.[6−8] The distribution of the hydrophobic moieties along the polymer backbone determines the behavior of the polymer in aqueous solution. Polymeric surfactants have a random distribution of amphiphilic segments and tend to form intramolecular aggregates, while associative polyelectrolytes and block copolymers mainly form intermolecular aggregates.[1,9]

The two amphiphilic polyelectrolytes used in this investigation are copolymers of two charged monomers, triethyl(vinylbenzyl)ammonium chloride and dimethyldodecyl(vinylbenzyl)ammonium chloride. The two polymers used, 40DT and 80DT, contain 40 and 80 mol % monomers with dodecyl side chains, respectively. These copolymers can be referred to as polysurfactants. Each amphiphilic unit is surfactant-like and contains both an alkyl chain and a polar cationic headgroup. Such copolymers exhibit solubility in water even for high content of amphiphilic groups, and the associative properties are controlled by the content and distribution of amphiphilic groups. Few studies of the interfacial behavior of these types of polyelectrolytes have been published. The forces acting between mica surfaces across a dilute solution of 40DT, one of the copolymers under our investigation, in 0.1mM KBr were monitored by Dedinaite et al.[10] The results indicate that the adsorbed layer formed consisted of an inner part that is strongly anchored to the surface and an outer part that is weakly attached to the inner layer.

One objective of the present study is to correlate bulk solution behavior with interfacial properties of amphiphilic

* To whom correspondence should be addressed.
[†] Lund University.
[‡] Royal Institute of Technology and Institute for Surface Chemistry.
[§] ESPCI-CNRS.

(1) Kötz, J.; Kosmella, S.; Beitz, T. *Prog. Polym. Sci.* **2001**, *26*, 1199−1232.
(2) Tribet, C.; Audebert, R.; Popot, J. L. *Langmuir* **1997**, *13*, 5570−5576.
(3) Yang, Y.; Engberts, J. B. F. N. *Colloids Surf., A: Physicochem. Eng. Asp.* **2000**, *169*, 85−94.
(4) Takahashi, M.; Kaneko, Y.; Arai, M. (Lion Corp., Japan). Jpn. Kokai Tokkyo Koho 2002322219, 2002, p 13.
(5) Benard, S.; Trouille, S.; Arnaud-Roux, M. (L'Oreal, Fr.) Eur. Pat. Appl. 1329470, 2003, p 14.
(6) Laschewsky, A. *Adv. Polym. Sci.* **1995**, *124*, 1−86.
(7) Morishima, Y. In *Solvents and self-organization of polymers*; Webber, S. E., Munk, P., Tuzar, Z., Eds.; Kluwer Academic Publishers: Dordrecht, 1996; pp 331−358.
(8) Cochin, D.; de Schryver, F. C.; Laschewsky, A.; van Stam, J. *Langmuir* **2001**, *17*, 2579−2584.
(9) Borisov, O. V.; Halperin, A. *Curr. Opin. Colloid Interface Sci.* **1998**, *3*, 415−421.

10.1021/la047311y CCC: $30.25
Published on Web 02/26/2005

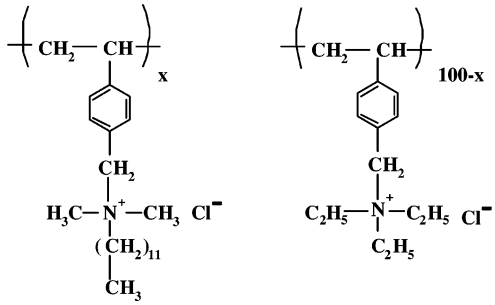

Figure 1. Monomer structures of the amphiphilic random polyelectrolytes used in this study: triethyl(vinylbenzyl)-ammonium chloride (right) and dimethyldodecyl(vinylbenzyl)-ammonium chloride (left).

copolymers at oppositely charged silica surfaces. Another is to elucidate how the graft density of hydrophobic side chains affects the interfacial layer. Based on the results obtained from the combination of the different techniques employed in this study, we will present a model of the bulk and interfacial behavior of 40DT and 80DT. The main technique used in this investigation is time-resolved ellipsometry, which is a nondestructive in situ technique and well suited for kinetic studies. It provides accurate measures of both average layer thickness and adsorbed amount with good time resolution. The adsorption studies were supplemented with investigations of the bulk behavior using dynamic light scattering and viscosity measurements.

2. Experimental Section

2.1. Materials. The two amphiphilic polyelectrolytes used in this investigation are random copolymers of two charged monomers, triethyl(vinylbenzyl)ammonium chloride and dimethyldodecyl(vinylbenzyl)ammonium chloride with molar weights of 254 and 366 g/mol, respectively (Figure 1). In the following we denote the polymers according to the fraction of monomers with hydrophobic dodecyl side chains: 40DT and 80DT contain 40 and 80 mol % monomers with hydrophobic side chains, respectively.

The polymers were obtained by quaternarization of a precursor, poly(vinylbenzyl chloride) (PVBC), according to the synthesis route of the analogous copolymer with hexadecyl side chains.[11] Briefly, the precursor PVBC was quaternarized in two steps in chloroform. First, the precursor, PVBC, was reacted with 40 or 80% dimethyldodecylamine, respectively. In the second step, the remaining vinylbenzyl chloride units of the precursor were quaternarized with triethylamine. The final copolymers were purified by precipitation in dimethyl ether, followed by dissolution in water and freeze-drying. This procedure is expected to result in random copolymers. The composition of the copolymers was confirmed by ^{1}H NMR of the partially quaternarized derivatives. The degree of polymerization and polydispersity of the precursor were estimated by size-exclusion chromatography in tetrahydrofuran. The number-average degree of polymerization is close to 100 ($DP_n \approx 100$), and the polydispersity $DP_w/DP_n \sim 2$, where DP_w is the weight-average degree of polymerization. Both copolymers have essentially the same polymerization degree and polydispersity. The molecular weights of these polyelectrolytes are 30 kDa for 40DT and ≈35 kDa for 80DT. The properties of the polyelectrolytes are summarized in Table 1.

Polymer stock solutions were prepared by dissolving the polymer powder in 10^{-4} or 0.1 M KCl solution to a final polymer concentration of 1000 ppm. The solutions were stirred for 2 days before each experiment and stored at a temperature of 10 °C until use.The water used in all experiments was deionized and passed through a Milli-Q filtration system (Millipore Corporation, Bedford, MA) with a pH of approximately 5.7 ± 0.2.

Table 1. Some Physical Properties of Polyelectrolytes Used in This Study

polymer	M_n (DP_n)	polydispersity M_w/M_n	d*n*/d*c* [mL/g]
40DT	29 900 (∼100)	2.0	0.154
80DT	34 400 (∼100)	2.0	0.156

The substrate used throughout this work was hydrophilic silica, prepared from polished silicon wafers (p-type, boron-doped, resistivity 1−20 Ω^{-1} cm) purchased from Okmetic Ltd. The silicon was thermally oxidized at 900 °C to obtain an oxide layer thickness of about 300 Å. The silicon wafers, cut into 2.0 × 1.2 cm slides, were cleaned in a 1:1:5 per volume mixture of 30 wt % H_2O_2, 25 wt % NH_4OH, and water at about 80 °C for 5 min. The slides were then rinsed with Millipore water. This was followed by cleaning in a 1:1:5 per volume mixture of 32 wt % HCl, 30 wt % H_2O_2, and water at about 80 °C for 10 min. After this procedure the slides were rinsed again with water and stored in 99 wt % ethanol. Before use the surfaces were dried in a nitrogen flow and cleaned for 5 min employing a radio frequency plasma (Harrick Scientific Corp., Model PDC-3XG) in residual air at a pressure of 0.03 mbar using a power input of 30 W. The resulting surface is hydrophilic as shown by contact angle measurements with water, giving contact angle values close to zero. The surface charge of the adsorbent, originating from dissociation of silanol groups, is negative and depends on the background electrolyte concentration (C_s) and pH with a point of zero charge at pH ≈2.[12]

2.2. Ellipsometry. The kinetics of the adsorption and desorption was followed in situ with ellipsometry, which allows accurate determination of both adsorbed amount (Γ) and layer thickness (d) with a time resolution of about 2 s. The measurements were performed with a modified, automated Rudolph Research thin-film null ellipsometer, Model 43603-200E, equipped with high precision stepper motors and controlled by a personal computer. The method and experimental setup are described in detail by Landgren and Jönsson.[13] The light source used was a xenon arc lamp, and the experiments were performed at a wavelength of 4015 Å at an angle of incidence, ϕ, of 68° under agitation with a magnetic stirrer in a temperature-controlled cuvette (25 ± 0.1 °C) equipped with plastic tubes that allowed continuous rinsing with salt solution.

The optical properties of the oxidized silicon substrate were obtained by measuring the ellipsometric angles Ψ and Δ in two ambient media,[13] in our case air and electrolyte solution. It is possible to calculate the complex refractive index ($N_2 = n_2 + jk_2$) of the bulk silicon, the thickness (d_1), and the refractive index ($N_1 = n_1$) of the silica layer. Typical values of these parameters are $n_2 = 5.5 \pm 0.01$, $k_2 = -0.35 \pm 0.03$, $d_1 = 300 \pm 20$ Å, and $n_1 = 1.48 \pm 0.005$, which may vary somewhat from batch to batch. Four-zone measurements were used at the beginning of each experiment to correct for imperfections in the optical components.[14] After characterization of the substrate, a known volume of the concentrated polymer solution ($C_p = 1000$ ppm) was injected into the trapezoid quartz cuvette, which originally contained 5 mL of KCl solution of the desired concentration, under intensive stirring (300 rpm) in order to obtain the desired polymer concentration. After injection of the stock solution, the changes in Ψ and Δ in one zone were recorded as a function of time until pseudoequilibrium was reached, i.e., until no further changes in ellipsometric angles with time were detected. For measurements of adsorption of 80DT in 100 mM KCl solutions, no steady state was achieved. All experiments were conducted for 25 h. In some of the experiments we performed rinsing with polymer-free salt solution once the measured Ψ and Δ had reached a steady state. Rinsing was performed at a continuous flow of 20 mL/min through the inlet of the tube, and the excess solutions were drained from the cuvette through the outlet of the tube, keeping the volume constant.

The recorded values of Ψ and Δ were evaluated using a four-layer optical model, assuming isotropic media and planar interfaces. The mean refractive index, n_f, and the ellipsometric

(10) Dedinaite, A.; Claesson, P. M.; Nygren, J.; Iliopoulos, I. *Prog. Colloid Polym. Sci.* **2000**, *116*, 84−94.
(11) Chassenieux, C.; Fundin, J.; Ducouret, G.; Iliopoulos, I. *J. Mol. Struct.* **2000**, *554*, 99−108.
(12) Iler, R. K. *The Chemistry of Silica*; Wiley: New York, 1979.
(13) Landgren, M.; Jönsson, B. *J. Phys. Chem.* **1993**, *97*, 1656−1660.
(14) Azzam, R. M. A., Bashara, N. M. *Ellipsometry and Polarized Light*; North-Holland: Amsterdam, 1989.

thickness, d_f, of the adsorbed layer were calculated using a numerical procedure described earlier.[15] From these values the adsorbed amount was calculated according to[16]

$$\Gamma = \frac{(n_f - n_0)d_f}{dn/dc}, \quad (1)$$

where Γ is the adsorbed amount, n_0 is the refractive index of the ambient bulk solution, and dn/dc is the refractive index increment of the polymer solution. The refractive index increments of each species used in this study were measured from aqueous solutions of different polymer concentrations at $\lambda = 5893$ Å using a Multiscale Automatic refractometer RFM-81 (BS, Tunbridge Wells, England) and then recalculated to $\lambda = 4015$ Å, as described by Mahanty and Ninham.[17] The dn/dc values for the polymers, which were found to be independent of the ionic strength under the conditions used in the present study, are given in Table 1.

The values of n_f and d_f are, as mentioned above, calculated under the assumption of layer uniformity. Since the adsorbed material in general is distributed in a nonhomogeneous manner normal to the surface, the calculations based on this model yield mean n_f and d_f values that must be interpreted with caution. We also note that the ellipsometer measures area of about 1 mm^2, which means that lateral inhomogeneities will be averaged out. For polymer systems, d_f tends to represent the inner dense part of adsorbed polymer layers and is expected to be lower than that determined by, for instance, light scattering or surface force measurements.[18−20]

2.3. Dynamic Light Scattering Measurements. The setup utilized for the dynamic light scattering (DLS) measurements is an ALV/DLS/SLS-5000F, CGF-8F based compact goniometer system from ALV-GmbH, Langen, Germany. The light source is a CW diode-pumped Nd:YAG solid-state Compass-DPSS laser with symmetrizer from COHERENT, Inc., Santa Clara, CA. It operates at 532 nm with a fixed output power of 400 mW. The laser intensity can be modulated by an external compensated attenuator from Newport Corporation. The instrument settings have been described in detail previously,[21] with the difference that the refractive index matching liquid used here was decalin instead of toluene. The temperature was controlled at 25 ± 0.01 °C. In this study the range of scattering angles was $22° \le \theta \le 135°$. The measured intensity fluctuations were analyzed using a regularized inverse Laplace transformation from which relaxation time distributions are obtained ($\tau A(\tau) = f(\log(\tau/\mu s))$, where τ is the relaxation time).[22,23] The relaxation rate (τ^{-1}) obtained from the first moment of the translation mode in the relaxation time distribution is used to estimate the translational mutual diffusion coefficient of the scattering polymers. In the limit of small scattering vectors, $\bar{q}$, the apparent translational diffusion coefficient (D) at finite concentration can be calculated from the relaxation rate τ^{-1} as $D = \tau^{-1}q^{-2}$, where $|\bar{q}| = (4\pi n/\lambda)\sin(\theta/2)$ is the magnitude of the scattering vector, n is the refractive index of the solvent, and θ is the scattering angle. In this system, the scattering particles are large ($qR_g \approx 1$), which causes D to be dependent on q. The value of D at $q = 0$ was therefore determined by extrapolating from a graph of $D = f(q^2)$. The apparent hydrodynamic radius is related to $D_{q=0}$ at finite polymer concentration through the Stokes−Einstein relationship:

$$R_H^{app} = \frac{kT}{6\pi\eta_0 D_{q=0}} \quad (2)$$

where k is Boltzmann's constant, T is the absolute temperature, η_0 is the viscosity of water, and $D_{q=0}$ is the diffusion coefficient at the zero angle. The relative error for both the diffusion coefficient and the hydrodynamic radius was estimated to be <5%.

2.4. Viscosity Measurements. The viscosity of the solutions of both polyelectrolytes was measured at different salt concentrations for $C_p = 0.05$ M repeating (cationic) units, which corresponds to 14.9 and 17.6 g/L for polymers 40DT and 80DT, respectively. The polymer solutions were prepared by dissolving the appropriate amount of solid polymer in NaCl solutions of different ionic strengths. All solutions were stirred (magnetic stirrer) at room temperature for, at least, 24 h before the measurements. Viscosity measurements were performed with a Low-Shear 30 apparatus (Contraves) at 25 °C. All solutions exhibited Newtonian behavior in the range of applied shear rates (<100 s^{-1}).

2.5. Tapping Mode AFM Imaging. Silica samples with adsorbed layers of 80DT obtained under different conditions (varying time of exposure, polyelectrolyte and salt concentration) were imaged by a Nanoscope III multimode SFM (Digital Instruments) operating in the tapping mode using an E tube scanner with a $10 \times 10(x,y) \times 2.5(z)$ μm scan range. The measurements were performed in air (relative humidity 25−60%) at room temperature (18−25 °C) not more than 10 h after the adsorption experiment was completed and the surface was removed from the solution. Microfabricated square pyramidal tips of etched single-crystal silicon with a bending spring constant of 42 N/m and a resonance frequency of 320 kHz (Pointprobes, Nanosensors GmbH) were used as received. The scan rate was 2 Hz, and images were obtained in the topographic mode. To eliminate imaging artifacts, the scan direction was varied to ensure that a true image was obtained. Images were obtained from at least five macroscopically separated areas on each sample. All images were processed using procedures for plane fitting and flattening using the Nanoscope IIIa software version 4.22 (Digital Instruments, Santa Barbara, CA) without any filtering.

3. Results

3.1. Aggregation in Solution. *3.1.1. DLS.* For aqueous solutions of 40DT (the polymer with fewer hydrophobic side chains), DLS measurements were performed at a finite concentration of 1000 ppm and at low ionic strength ($C_s = 10^{-4}$ M KCl) as well as lower polymer concentration, but the scattering intensity was too low to obtain good statistics. The DLS measurement for $C_p = 1000$ ppm and $C_s = 0.1$ M KCl, performed at $\theta = 90°$, gave a single-exponential correlation function with a characteristic relaxation time, which corresponds to $D_{q=0} = 6 \times 10^{-11}$ m^2/s, and from eq 2 $R_H^{app} = 36$ Å. This value should be close to the true R_H under these dilute conditions. A preliminary measurement at $C_p = 200$ ppm returned a similar size (data not shown). From these results we conclude that there are only unimolecular micelles built from a single polyelectrolyte chain present in the solution, but no aggregates of unimolecular micelles. If we assume that the shape of the unimolecular micelle is close to spherical, where the dodecyl chains of the polymer are in the core and the triethylammonium groups are oriented toward the aqueous phase, we can estimate its dimension from tabulated bond lengths and angles. The triethyl(vinylbenzyl)ammonium and dimethyldodecyl(vinylbenzyl)ammonium groups extend to 11 and 24 Å, respectively, from the polymer backbone. The dodecyl chains are expected to form the core of the unimolecular micelle, and due to packing constraints some of the triethyl(vinylbenzyl) groups have to be on the surface. The maximum radius of the unimolecular micelle can thus be estimated to be 35 Å, which is similar to the value observed in the DLS

(15) Tiberg, F.; Landgren, M. *Langmuir* **1993**, *9*, 927−932.
(16) De Feijter, J. A.; Benjamins, J.; Veer, F. A. *Biopolymers* **1978**, *17*, 1759−1772.
(17) Mahanty, J.; Ninham, B. W. *Dispersion Forces*; Academic Press: London, 1976.
(18) Claesson, P. M.; Blomberg, E.; Paulson, O.; Malmsten, M. *Colloid Surf., A: Physicochem. Eng. Asp.* **1996**, *112*, 131−139.
(19) Nylander, T.; Wahlgren, N. M. *Langmuir* **1997**, *13*, 6219−6225.
(20) Kull, T.; Nylander, T.; Tiberg, F.; Wahlgren, N. M. *Langmuir* **1997**, *13*, 5141−5147.
(21) Jansson, J.; Schillen, K.; Olofsson, G.; da Silva, R. C.; Loh, W. *J. Phys. Chem. B* **2004**, *108*, 82−92.
(22) Jakes, J. *Collect. Czech. Chem. Commun.* **1995**, *60*, 1781−1797.
(23) Schillén, K.; Brown, W.; Johnsen, R. M. *Macromolecules* **1994**, *27*, 4825−4832.

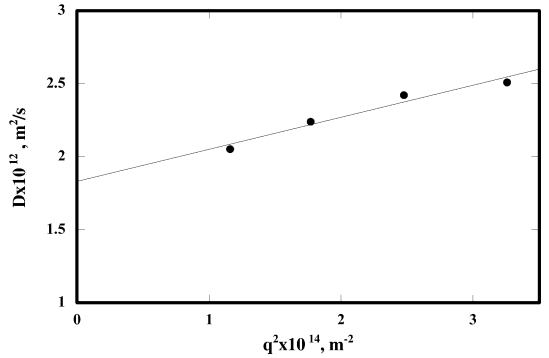

Figure 2. Apparent translational diffusion coefficient, D, plotted versus square of the scattering vector, q^2, from DLS of a solution containing 50 ppm 80DT in 0.1 M KCl.

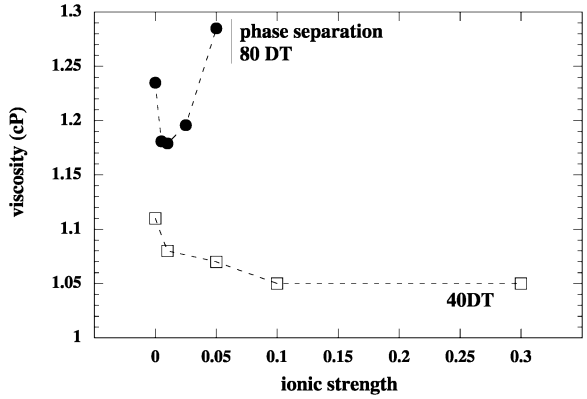

Figure 3. Viscosity of 40DT and 80DT solutions as a function of ionic strength. The polymer concentration is 0.05 M in repeating units, which corresponds to 14.9 and 17.6 g/L for polymers 40DT and 80DT, respectively.

experiment, 36 Å. We note that the measured hydrodynamic radius for the unimolecular micelles suggests that there is only one hydprophobic domain (core) formed from a single polymer chain. This is a consequence of the relatively short backbone of the polymers used. For large polymers, each polymer can have several unimolecular micelles.[7]

The DLS measurements were also performed on the aqueous 80DT solutions containing 0.1 M KCl. The relaxation time distributions obtained from the data analysis were found to be monomodal with a single relaxation mode positioned at a larger relaxation time compared to the 40DT case (see above). We attribute this single mode to the translational diffusion of intermolecular aggregates. No evidence of single polymer chains was observed in the relaxation time distributions. Here it should be borne in mind that the relaxation time distribution is dominated by the scattering from the aggregates because it is an intensity-weighted distribution. For the dilute 80DT solution, $D_{q=0}$ is obtained by extrapolation to zero angle. The results are presented in Figure 2. Since the polymer concentration in our experiment is very low (50 ppm), we assume that the calculated R_H^{app} is close to the true R_H. The value of the diffusion coefficient obtained for 50 ppm 80DT solution, $D_0 = (1.8 \pm 0.1) \times 10^{-12}$ m^2 s^{-1}, corresponds to $R_H = 1300$ Å. On the basis of this value, we conclude that the observed scattering arises from intermolecular aggregates in the solution. They are suggested to be formed by an attractive interaction between dodecyl chains grafted to different polymer molecules.

3.1.2. Viscosity Data. Figure 3 shows the viscosity data for 40DT and 80DT at different ionic strengths. The

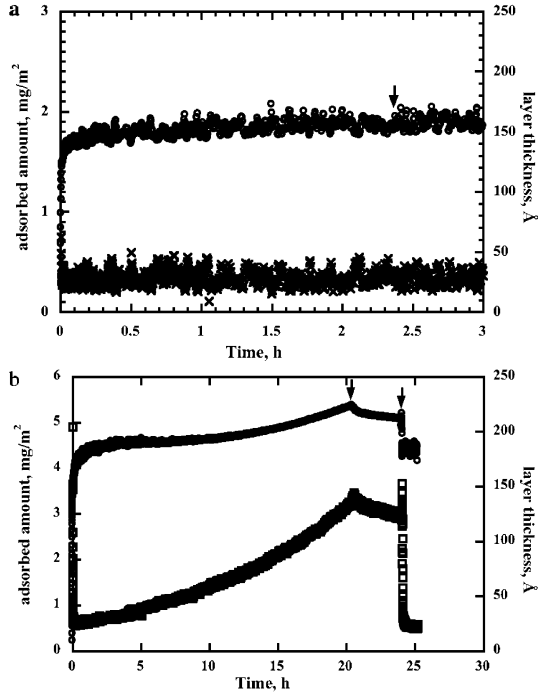

Figure 4. (a) Effect of rinsing on adsorbed layer characteristics of 40DT adsorbed from a solution of 50 ppm polymer in 0.1 M KCl. The arrow indicates rinsing by polymer-free solution of 0.1 M KCl. (b) Effect of rinsing on adsorbed layer characteristics of 80DT adsorbed from a solution of 50 ppm polymer and 0.1 M KCl. The first arrow indicates rinsing by polymer-free solution of 0.1 M KCl, and the second arrow indicates rinsing with water. (○) Adsorbed amount; (×) layer thickness.

concentration of the polymers was held constant (0.05 M repeating units, corresponding to 1.5 and 1.75 wt % 40DT and 80DT, respectively). We can clearly see that the effect of salt on the rheological behavior is very different for 40DT and 80DT. At low salt concentrations (up to approximately 0.01 M) the relative viscosity decreases for both polymers. This feature reflects the fact that upon increasing the concentration of electrolyte the repulsion between the charged segments is screened and the polymer chains become less rigid. This facilitates the assembly of dodecyl groups and formation of unimolecular micelles. Thus, the density of the micellar core increases with salt concentration. At higher electrolyte concentrations, the viscosity of 40DT solutions continues to decrease and then becomes relatively insensitive to electrolyte concentration at about 0.1 M added salt. In this respect 40DT behaves like a typical polysoap.[9] Here it should be pointed out that the rigid styrene backbone imposes a limit on how small the unimolecular micelles can be. No phase separation is observed in the 40DT system for salt concentrations up to at least 0.5 M.

The behavior of 80DT at high salt concentration (starting from 0.01 M) is opposite that of 40DT, and the viscosity increases with salt concentration, similar to that of an associative polyelectrolyte, where intermolecular forces determine the rheological properties.[1] Above 0.05 M added electrolyte the polymer solution phase separates. Here we note that no visible phase separation was observed for solutions of lower polymer concentration (50 ppm) at 0.1 M KCl, which we used for DLS and ellipsometry measurements, but clearly our dilute system approaches the limit of phase separation. This explains the presence of intermolecular aggregates in the DLS measurements.

3.2. Kinetics of Adsorption. Figure 4a gives a typical example of the time dependence of the adsorbed amount

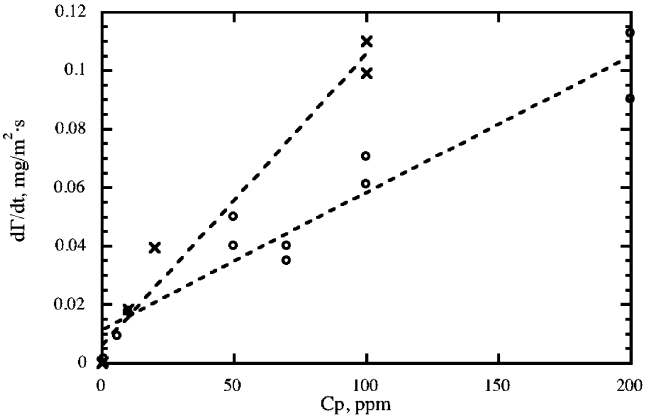

Figure 5. Initial rates of adsorption at 0.1 M KCl for 40DT (×) and 80DT (○) as a function of bulk concentration.

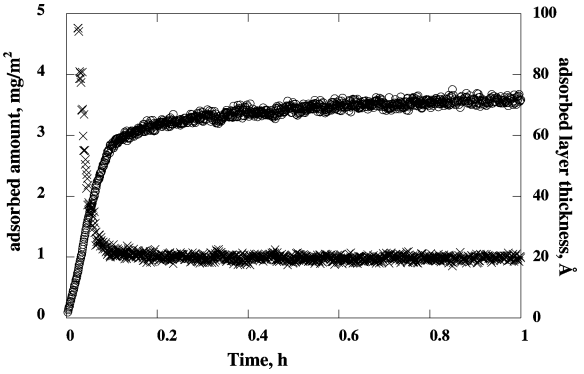

Figure 6. Time dependence of adsorption during the first hour.The example given is for a solution of 80DT with a concentration of 6 ppm at 0.1 M KCl. Adsorbed amount (○) and layer thickness (×) are given.

and the adsorbed layer thickness measured during adsorption of 40DT from a solution with a polymer concentration of 50 ppm in 0.1 M KCl. After the injection of the polymer stock solution into the ellipsometry cuvette, a sharp increase in the adsorbed amount is observed within the first few minutes, and then the adsorbed amount approaches an apparent plateau value within approximately 2 h. The initial adsorption rate is very high at this concentration of the polymer, and the adsorbed amount initially increases linearly with time.

Qualitatively, the kinetics of the adsorption process showed three different stages: a rapid increase in adsorption within the first few minutes, followed by a slower approach to a plateau level, and a steady state of the process. The adsorption mechanism can be thought of as a three-step process: (i) transport from the bulk to the surface, (ii) attachment to the surface, and (iii) rearrangements in the adsorbed layer. The adsorption rate is transport-limited when all polymer that arrives at the surface adsorbs immediately. For diffusion-controlled adsorption the transport rate $d\Gamma/dt$ through the stagnant layer can in the simplest case be modeled as[24]

$$\frac{d\Gamma}{dt} = \frac{D}{\delta} C_p \qquad (3)$$

Here D is the polymer diffusion coefficient and δ is the thickness of the stagnant layer, which for the cuvette geometry and stirring rate used has been estimated to be 100 μm.[25] As is obvious from eq 3, we expect the adsorption rate to be proportional to the polymer concentration.

This is apparent in Figure 5, where the initial adsorption rate is plotted against the bulk polymer concentrations for 40DT and 80DT in 0.1 M KCl. Using the slopes of the linear fits from Figure 5, the diffusion coefficients were estimated to be smaller than $\sim 10 \times 10^{-11}$ m^2/s for 40DT and $\sim 5 \times 10^{-11}$ m^2/s for 80DT. The diffusion coefficient measured by DLS for 40DT at the same salt concentration was $\sim 6 \times 10^{-11}$ m^2/s, which is within a factor of 2 of the one estimated from the initial adsorption rate. In the 80DT case, the DLS measurements did not give us information on the unimicellar diffusion coefficient and a comparison is therefore not possible.

The second stage of the adsorption process is considerably slower because adsorption is hindered due to the steric and electrostatic barriers that arriving molecules encounter. At this stage, which occurs at intermediate surface coverage, the rate of adsorption also depends on the attachment process. For even higher surface coverage, the rate of adsorption no longer depends on the transport of molecules to the surface. It should be noted that the attachment-limiting regime of adsorption continues on a much longer time scale for both polymers when the electrolyte concentration is low, 10^{-4} M KCl (data not shown). For the adsorption of polymers 40DT and 80DT from a solution containing 0.1 M KCl, the plateau coverage is approached within the first half hour, whereas for the same two polymers at the same concentration but in the presence of 10^{-4} M KCl it takes ~3 h or more to approach steady state. This is due to the higher electrostatic barrier at low ionic strength, which hampers the attachment process.

We would like to emphasize another interesting feature connected to the kinetic aspects of the adsorption of the amphiphilic polyelectrolytes on silica. Figure 6 shows the time dependence of adsorption during the first hour from an 80DT solution with 0.1 M KCl and a polymer concentration of 6 ppm. Here we note that we observed qualitatively the same behavior during the initial adsorption process, irrespective of the degree of polymer hydrophobic modification and ionic strength. Initially, the thickness of the adsorbed layer is high (for the example given in Figure 6, it is above ~100 Å), but decreases rapidly with time as the coverage of the surface approaches the steady-state value (~20 Å in the given example).

3.3. Adsorption Isotherms at Different Ionic Strengths. Adsorption isotherms recorded at 25 °C for the 40DT polymer in the presence of 10^{-4}, 0.1, and 1 M KCl and for the 80DT polymer in 10^{-4}, 0.01, and 0.1 M KCl are shown in Figure 7. Here, each point was obtained from a separate set of adsorption experiments. Generally, high-affinity-type adsorption isotherms were obtained for both polymers at all ionic strengths, where the adsorption reaches the plateau value at concentrations below 50 ppm, except for 80DT at 0.1 M KCl (discussed below).

At low ionic strength, very thin adsorbed layers were observed for both polyelectrolytes, with values of the average thickness that are below 2−5 Å (see Figure 8a). It should be noted that the plateaus of the adsorbed amounts at this low ionic strength (10^{-4} M KCl) are low, 0.45 ± 0.1 mg/m^2 and 0.6 ± 0.1 mg/m^2 for 40DT and 80DT, respectively. The conformation of the polyelectrolyte is expected to be extended and rodlike with the polymer chain stretched parallel to the surface. Intermolecular interactions are expected to increase with the degree of hydrophobic modification, which in turn is expected to result in a thicker layer. However, the average layer thickness of 40DT for a polymer concentration of 100 ppm

(24) Cuypers, P. A.; Willems, G. M.; Kop, J. M. M.; Corsel, J. W.; Janssen, M. P.; Hermens, W. T. *ACS Symp. Ser.* **1987**, *343*, 208−221.
(25) Tiberg, F.; Jönsson, B.; Lindman, B. *Langmuir* **1994**, *10*, 3714−3722.

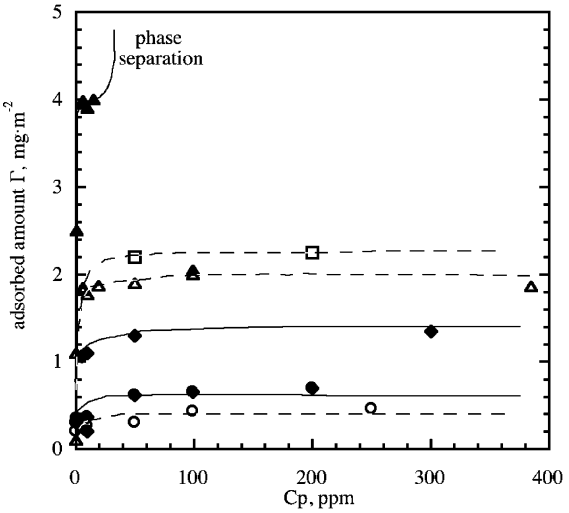

Figure 7. Adsorption isotherms for 40DT at 10^{-4} M KCl (○), 0.1 M KCl (△), and 1 M KCl (□) and for 80DT at 10^{-4} M KCl (●), 0.01 M KCl (◆), and 0.1 M KCl (▲). Lines are added only to guide the eye.

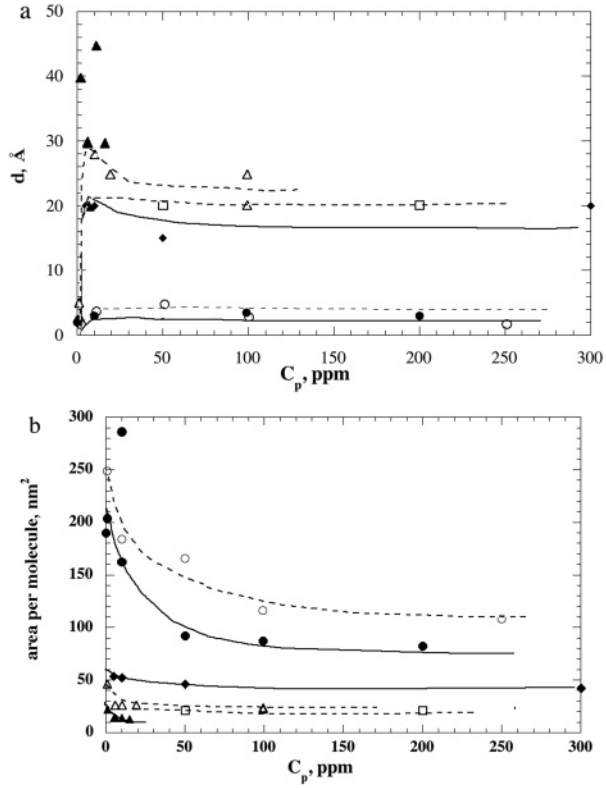

Figure 8. (a) Average adsorbed layer thickness and (b) area per adsorbed molecule versus bulk concentration for 40DT at 10^{-4} M KCl (○), 0.1 M KCl (△), and 1 M KCl (□) and for 80DT at 10^{-4} M KCl (●), 0.01 M KCl (◆), and 0.1 M KCl (▲). Dashed lines (for 40DT) and solid lines (for 80DT) are added only to guide the eye.

is found to be approximately 2 Å and for the same concentration of 80DT the obtained value is 3 Å, but this small difference is insignificant as we cannot determine the thickness to a high enough degree of accuracy at such a low adsorbed amount. We also note that the layer formed under these conditions most likely is patchy since the number of charges brought to a small area of the surface by a polymer exceeds the number of charged sites on this surface area (see discussion below). Thus, the small ellipsometric thickness, which is an average over a large surface area, is expected to underestimate the thickness of the adsorbed polymer.

Let us take into account the small difference in the number of cationic units, brought to the surface by 1 mg of each polyelectrolyte. That is, if we replot the adsorption isotherm in micromoles of cationic units per square meter, the adsorption isotherms for 40DT and 80DT at 10^{-4} M KCl almost coincide. For example, 0.45 mg/m^2 corresponds to 1.51 μmol of cationic units/m^2 for 40DT, and 0.6 mg/m^2 corresponds to 1.75 μmol of cationic units/m^2 for 80DT. The results suggest that the electrostatic interactions with the surface dominate the adsorption process, while the degree of hydrophobicity of the polymers is rather insignificant at low ionic strength. On the other hand, at higher electrolyte concentration, the adsorption behavior of the polymers is very different and the degree of polymer hydrophobicity has a significant effect.

For 40DT, an increase of the salt concentration from 10^{-4} to 0.1 M KCl has a dramatic effect on the adsorbed amount and the layer thickness. The average layer thickness is 20 Å at the plateau (see Figure 8a), which is approximately 10 times higher than the thickness obtained in the presence of 10^{-4} M KCl. The adsorbed amount at the plateau is 1.9 ± 0.1 mg/m^2, or 5.4 μmol of cationic units/m^2, which is more than 4 times higher than that at the lower salt concentration. This gives a high density of the adsorbed layer, 0.95 g/cm^3. A further increase of the ionic strength to 1 M KCl has only a minor effect on the adsorption of 40DT, as the layer thickness is the same as at 0.1 M KCl, 20 Å, and the adsorbed amount is only 15% higher (Figure 8a).

For 80DT, the increase in salt concentration from 10^{-4} to 0.01 M KCl also promotes the adsorption. The average layer thickness is about 20 Å at the plateau, and is approximately 10 times higher than the thickness obtained in the presence of 10^{-4} M KCl. The adsorbed amount at the plateau is 1.3 ± 0.1 mg/m^2, or 3.78 μmol of cationic units/m^2, which is more than 2 times higher than that at the lower salt concentration, and the density is 0.65 g/cm^3. In contrast to 40DT, the adsorption of 80DT increases dramatically when the ionic strength is increased further to 0.1 M. In addition, the adsorption isotherm for 80DT in the presence of 0.1 M KCl features a semiplateau at the polymer concentrations of 5−15 ppm. The thickness of the adsorbed layer obtained is constant for low concentrations of the polymer, about 25 ± 5 Å, which is practically the same value as in the presence of 0.01 M KCl. However, the adsorbed amount for the same concentration of the polymer is substantially higher, which means that the chains are more closely packed at higher salt concentration. A further increase in the polymer concentration to C_p = 15 ppm gives a significantly thicker layer (50 Å).

At 80DT concentrations of 50 ppm and higher, we do not reach a plateau value of the adsorbed amount as illustrated in Figure 9. Instead, the adsorbed amount first increases sharply with time for any given polymer concentration. The layer then seems to reach a pseudo-plateau, where the adsorbed amount and the layer thickness change only slightly with time for about 0.5−1 h, depending on concentration. After this lag phase a further increase in both thickness and adsorbed amount with time is observed. These data indicate the formation of a multilayer polymer film. Obviously this is the characteristic of a system close to the phase separation limit, although the solution seems to be transparent on visual inspection. The data shown in Figure 3 confirm that macroscopic phase separation occurs at higher polymer concentration if the ionic strength is increased above 0.05 M.

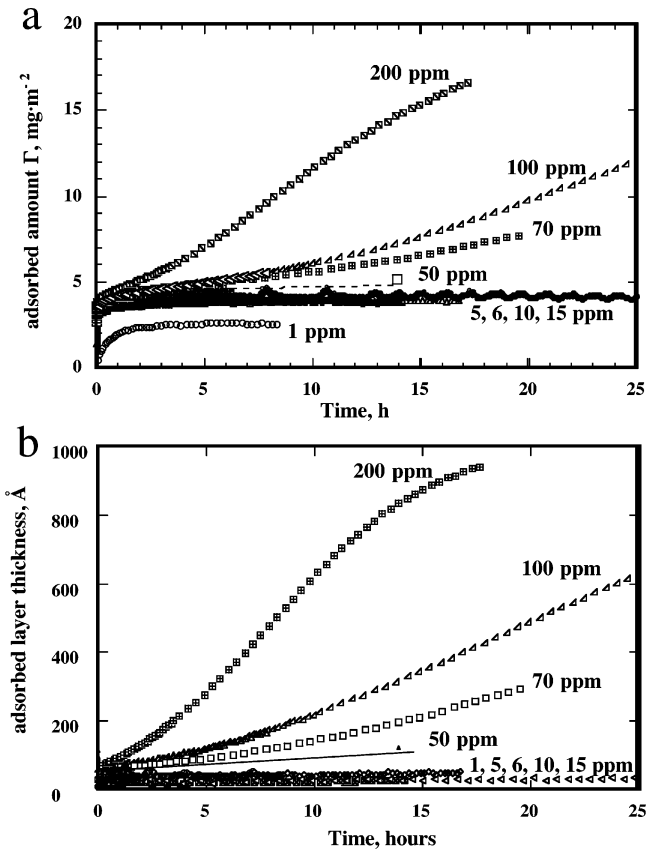

Figure 9. (a) Adsorbed amount and (b) adsorbed layer thickness versus time for different equilibrium polymer concentrations of 80DT at 0.1 M KCl.

3.4. Effect of Rinsing on Adsorbed Layer Characteristics. Figure 4 gives two distinct examples of the effect of rinsing on the adsorbed layer characteristics of 40DT and 80DT, adsorbed from a solution with the same polymer and salt concentrations (C_p = 50 ppm and C_s = 0.1 M). In the first example (Figure 4a), the cuvette was flushed with a polymer-free solution containing 0.1 M KCl after about 2.3 h of adsorption of 40DT. No desorption or change in the layer thickness was observed during the time scale of the experiment (sometimes several hours). It should be noted that flushing the cuvette with pure water instead of salt solution had the same effect; i.e., no change in the adsorbed layer was noticed. In the second example (Figure 4b), the cuvette was flushed with a polymer-free solution containing 0.1 M KCl after about 20.5 h of adsorption of 80DT. In this case the rinsing was started even though the adsorption did not reach steady state. Here we observed that a few percent of material accumulated on the surface was desorbed during 4 h of rinsing, which indicates that desorption occurs but the rate of this process is quite slow. However, if rinsing with water was performed after ≈24 h, the adsorbed amount and the layer thickness were rapidly and substantially reduced to a level that remained constant even after several hours of rinsing. The remaining layer corresponds approximately to the coverage achieved at low 80DT concentrations (1−15 ppm), which was found to correspond to a monolayer coverage of the polymer, as discussed below.

3.5. Aggregation at the Interface. The aggregates formed upon adsorption of 80DT on silica from the aqueous solutions containing 0.1 M KCl were observed directly by AFM. Films produced in the ellipsometry cuvette were dried and saved for further analysis. Tapping mode AFM images of the dry polymer 80DT films after adsorption

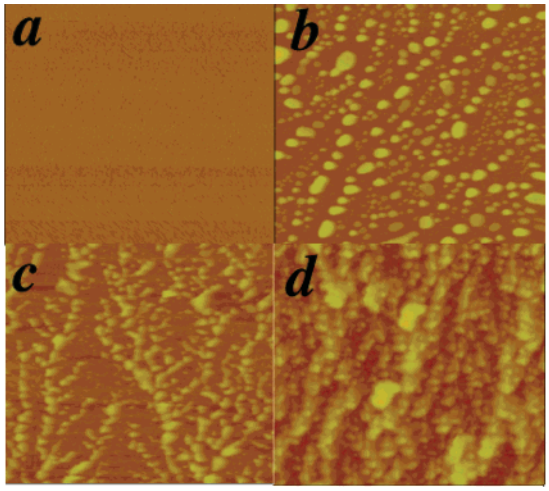

Figure 10. Topographic AFM images of dry 80DT films after adsorption in 0.1 M KCl. Scanned area is 10 × 10 μm. (a) z range 28 nm. C_p = 1 ppm; corresponding to Γ = 2.6 mg/m^2 and d = 35 Å measured by ellipsometry. (b) z range 500 nm. C_p = 50 ppm; corresponding to Γ = 5.2 mg/m^2 and d = 120 Å measured by ellipsometry. (c) z range 500 nm. C_p = 70 ppm; corresponding to Γ = 7.8 mg/m^2 and d = 300 Å measured by ellipsometry. (d) z range 500 nm. C_p = 100 ppm; corresponding to Γ = 13 mg/m^2 and d = 700 Å measured by ellipsometry.

from 0.1 M KCl solution at the silica surface are collected in Figure 10 and reveal the morphology of the surface films. The images show a growth in the lateral density of aggregated domains with exposure time and/or with polyelectrolyte concentration. The surface topography images demonstrate formation of rough and inhomogeneous films with the thicker domains increasing in size with larger ellipsometric thickness. Note that the features observed in the AFM images do not correspond to single aggregates, but rather to clusters of them, which are varying in size. In general, the roughness increases with the increase of the adsorbed amount. One might question if the observed roughness is not a consequence of the drying process. Therefore, we also imaged the aggregates on the surface in a solution containing 100 ppm 80DT and 0.1 M KCl employing the liquid cell AFM using soft-contact mode. The image shows an inhomogeneous film with roughly circular domains varying in size (100−500 nm), quite similar to those observed on the dried film (data not shown). Here we note that the measurements in the liquid cell are much more complicated and the images obtained are more fuzzy because we need to use weaker forces in order to not affect the film. Thus, once the correlation between the structure of wet and dried film topography was established, we preferred to work with dried films.

4. Discussion

4.1. Formation of a Polymer Monolayer. Regarding the kinetics of adsorption, we can conclude that the first stage of adsorption, encountered at low surface coverage and short adsorption times (Figure 4a), represents a diffusion-controlled regime. The rearrangements in the adsorbed layer observed during the initial stage of the adsorption process as a decrease in the layer thickness (Figure 6) corresponds to the initial linear increase of the adsorbed amount with time. This shows that the rate of rearrangements is similar to the rate of adsorption. A large dimensional change of the interfacial layer is expected if we consider that both 40DT and 80DT are highly positively charged, and therefore tend to stretch out at the interface in order to effectively compensate the surface charge. Similar types of rearrangements were

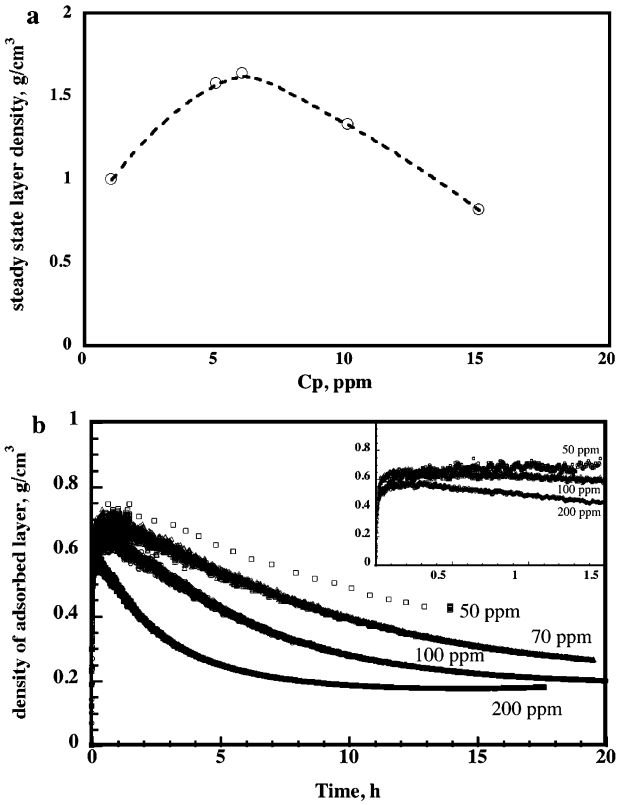

Figure 11. Density of adsorbed 80DT layer in 0.1 M KCl. (a) Density of adsorbed layer corresponding to steady state at low polymer concentrations; (b) kinetic evolution of adsorbed layer density for 50−200 ppm bulk concentration of 80DT. Insert shows the same data for shorter times, <1.5 h.

observed during adsorption of hydrophobically modified polyacrylates on hydrophobic surfaces, also using time-resolved ellipsometry.[26] In that study it was found that a polymer that does not associate in solution tends to optimize the interaction between the polymer hydrophobic groups and the hydrophobic surface. This process results in "spreading" of the polymer molecules at the interface. A similar process occurs in our case, but here the driving force for spreading is electrostatic.

The area per adsorbed molecule, assuming isolated chains on the surface, is plotted against the polymer concentration for both polymers at different ionic strengths in Figure 8b. The main conclusions from these data are that (i) the area per molecule is, of course, decreasing with the polymer concentration until the plateau value is reached and (ii) the polymer molecule occupies a rather large area at low salt concentration, which can be explained by repulsive electrostatic interactions between the charged segments that lead to conformations of the polymer molecule that are extended and lying flat on the surface.

For electrostatically driven adsorption, the net charge of the substrate surface and the charge brought to the surface by the adsorbing species are expected to compensate each other stoichiometrically. For an electrolyte concentration of 10^{-4} M and pH ~5.6, the number density of dissociated silanol groups on silica is approximately 0.017 SiO^- group/nm^2.[27] If we use these data and the adsorbed amount from Figure 7, we find that there are about 2 negative charges per adsorbed polymer molecule, which carries 100 positive charges. The overcompensation of the silica charge will therefore be large, by a factor of roughly 50 for both polymers at this salt concentration. At a higher salt concentration, 0.1 M, the corresponding density of SiO^- groups is roughly 0.07/nm^2. Under these conditions the surface charge will be overcompensated by a factor of 50 by adsorbed 40DT, and for 80DT in the concentration range of 5−15 ppm this value reaches 100. At higher 80DT concentrations, the overcompensation of the underlying silica charges will be even more over time. For instance, after 15 h of 80DT adsorption from 200 ppm solution, this value reaches 400. In these simple calculations, we assume that the number of dissociated SiO^- groups is independent of the polymer adsorption. It is known, however, that adsorption of cationic polyelectrolyte onto charge-regulating surfaces like silica induces additional dissociation of functional groups at the surface. The number of titratable charges on silica, therefore, increases in the presence of polycations,[28] and the overcompensation of the charge as calculated above is an overestimation. Let us consider the unlikely limiting case where all surface silanols are ionized due to adsorption of the cationic polyelectrolyte. The maximum density of ionizable silanol groups is 3.1 sites/nm^2 according to Yates and Healy,[29] as measured by the tritium exchange procedure. To obtain stoichiometric charge compensation between the adsorbed polymer and surface, between 50% and 100% of all silanol groups on the silica surface need to be dissociated, depending on electrolyte concentration. For the bare silica only 0.5−2% of the silanol sites are dissociated under the conditions studied. Our previous results suggest that adsorption of a polyelectrolyte on silica particles does not have a sufficiently large effect to dissociate all or even 50% of the silanol groups.[30]

The reason for the observed overcompensation could be that, in addition to electrostatic interactions, nonelectrostatic interactions also contribute to the adsorption free energy. In particular, for the hydrophobically modified polymer at high ionic strength, where the range of the electrostatic forces is diminished, reducing the contact between the aqueous solution and the hydrophobic dodecyl side chains on the polymer is expected to favor adsorption. This will compensate the effect of the repulsive electrostatic forces within the layer, which arises from charge accumulation in the interfacial region. Another reason for the overcompensation of the surface charge could originate from the fact that the charges on the polymer are discrete and connected. Our simple calculation of charge compensation does not take into account the geometry in the real system. Therefore, charge overcompensation can occur when the distance between the charges on the polymer chain is smaller than that between the surface charges. This view has been put forward before and has received support in a number of experimental studies.[31−33] In our case, the charges are localized on the side chains with a distance from the backbone of 7.5 Å. If we consider the polymer to be adsorbed in an extended conformation parallel to the surface, where the side chains extend randomly from both sides of the polymer backbone,

(26) Poncet, C.; Tiberg, F.; Audebert, R. *Langmuir* **1998**, *14*, 1697−1704.
(27) Bolt, G. H. *J. Phys. Chem.* **1957**, *61*, 1166.
(28) Shubin, V.; Linse, P. *Macromolecules* **1997**, *30*, 5944−5952.
(29) Yates, D. E.; Healy, T. W. *J. Colloid Interface Sci.* **1976**, *55*, 9−19.
(30) Samoshina, Y.; Nylander, T.; Shubin, V.; Bauer, R.; Eskilsson, K. Submitted for publication in *Langmuir* **2004**.
(31) Eriksson, L.; Alm, B.; Stenius, P. *Colloid Surf., A: Physicochem. Eng. Asp.* **1993**, *70*, 47−60.
(32) Hoogeveen, N. G.; Stuart, M. A. C.; Fleer, G. J. *Colloid Surf., A: Physicochem. Eng. Asp.* **1996**, *117*, 77−88.
(33) Shubin, V.; Samoshina, Y.; Menshikova, A.; Evseeva, T. *Colloid Polym. Sci.* **1997**, *275*, 655−660.

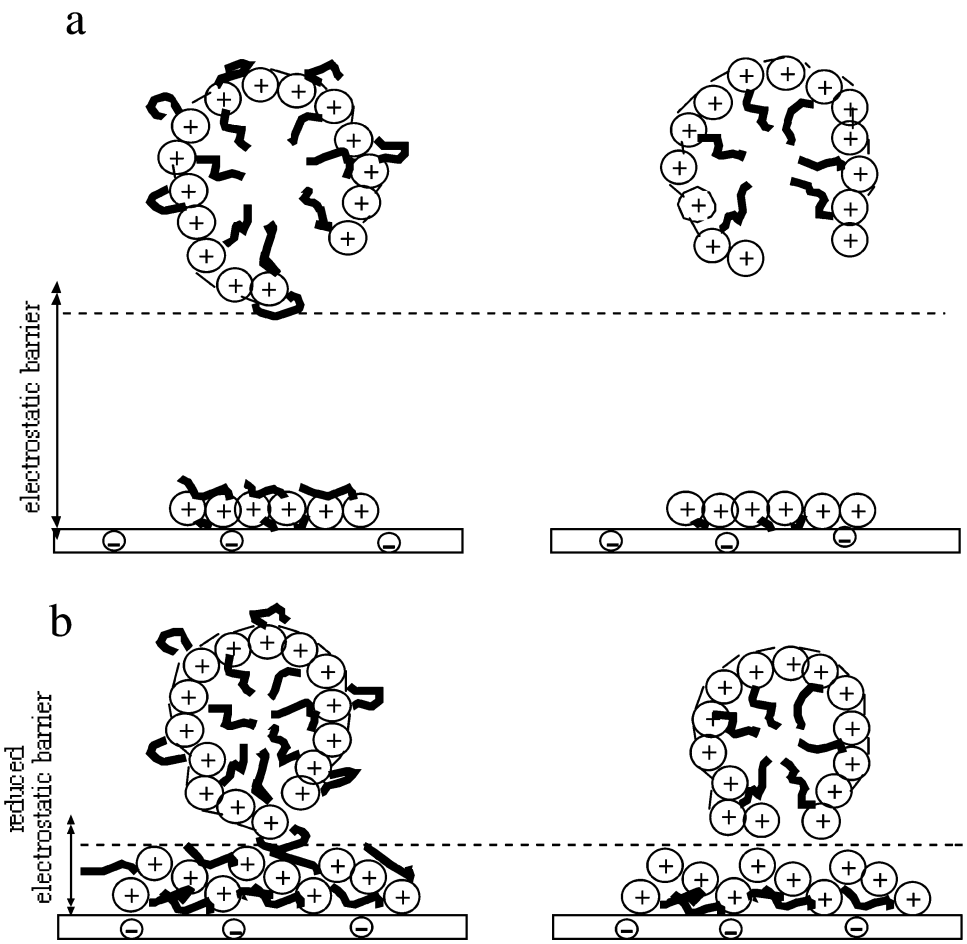

Figure 12. Schematic picture of bulk and interfacial behavior of 40DT (right) and 80DT (left) at (a) low ionic strength and (b) high ionic strength.

then the distance between the positive charges along the polymer chain will be ~5 Å, and for two charges on opposite sides of the backbone it will be about ~15 Å. The mean distance between charges then will be ~8 Å. If we compare this value with the mean distance between surface SiO^- groups of 30−70 Å, expected for the electrolyte concentrations and pH used in the present study, it is obvious that the charges of the adsorbed polymer molecule cannot match the surface charges. However, there are several examples of situations where linear highly charged polyelectrolytes adsorb to moderate charge density surfaces such as silica and glass without causing the large overcompensation found in this study (see, e.g., Poptoshev et al.[34]). It has also been noted that branched polyelectrolytes overcompensate the surface charge more than linear ones (cf. ref 35), but not to the degree found in the present study.

No desorption of polyelectrolytes on rinsing was observed in any case of 40DT and 80DT adsorption irrespective of bulk concentration or ionic strength, except for 80DT at bulk concentrations above 15 ppm in 0.1 M KCl. These results reveal an apparent irreversibility of the adsorption of highly charged cationic polymers onto the negatively charged silica surface with respect to dilution, which confirms the high affinity of the polymers for the surface.

4.2. Formation of Polymer Aggregates at the Surface. We will now focus our discussion on the mechanisms that control the formation of the polymer multilayers. For this purpose, we show the variation in the density of adsorbed 80DT polymer layers in 0.1 M KCl; see Figure 11. Figure 11a shows the plateau values of the layer density versus polymer concentration in the range of 1−15 ppm. First, up to a 80DT concentration of 7 ppm the density of the adsorbed layer increases with bulk polymer concentration, while the thickness remains constant. At higher bulk polymer concentrations, the layer starts to expand and the density decreases. This is suggested to be due to electrostatic repulsion within the layer.

Figure 11b illustrates the evolution of the layer density with time for higher bulk concentrations (50−200 ppm). During the initial stages of adsorption, the density of the adsorbed layer increases sharply with time until it reaches a maximum, which is approximately the same, ~0.65 g/cm^3 for the whole range of these concentrations. This corresponds to the apparent steady state of adsorption (lag phase) achieved in the time range ~0.3−0.5 h (depending on C_p) after injection of the polymer solution. For this stage, the mean values of the surface excess and the average thickness were approximately the same for all polymer concentrations, that is, 4.1 mg/m^2 and 60 Å, respectively (cf. Figure 9). This quasi-steady state is extended for lower bulk concentrations, and the higher the concentration of the polymer, the less broad the maximum that is observed.

The observation of a maximum in density suggests that (close to) full monolayer coverage has been reached, which is limited by the repulsion between charged polymer

(34) Poptoshev, E.; Rutland, M. W.; Claesson, P. M. *Langmuir* **1999**, *15*, 7789−7794.
(35) Poptoshev, E.; Claesson, P. M. *Langmuir* **2002**, *18*, 2590−2594.

segments. After the maximum, the density decreases and seems to approach a constant value of ~0.2 g/cm^3 after very long time. The rate of the density decrease depends on the polymer concentration (Figure 11b); i.e., the higher the concentration of the polymer, the higher the rate of density decrease that is observed. For example, half the maximum density is achieved for a bulk concentration of 200 ppm within ~2.5 h, whereas for a bulk concentration of 100 ppm it takes ~7.5 h. The fact that we observe a decrease in layer density, while both the adsorbed amount and the average thickness increase, means that the layer thickness is expanding faster than accounted for solely by the adsorbed mass, which in turn reflects that a nonhomogeneous layer has been formed, as confirmed by the AFM images.

What is then the driving force for additional polymer to adsorb to a surface already covered with polymer? Our interpretation is that the surface becomes less polar, since at high density of grafted hydrophobic dodecyl side chains on the polymer some of these chains are exposed on the surface due to packing constraints. In 0.1 M KCl, the electrostatic barrier caused by the surplus of charge in the layer can be overcome and the hydrophobic interactions between dodecyl segments present in the adsorbed layer and on the polymer molecules in bulk facilitate the buildup of aggregates at the surface. We also note that this layer could be removed by rinsing with pure water, leaving only a monolayer on the surface (Figure 4b). Clearly, the lowering of the ionic strength increases the electrostatic repulsion within the layer, which triggers the desorption of the outer part of the layer, leaving only the innermost layer that is most strongly attached to the surface.

The adsorption data demonstrating multilayer formation for 80DT at 0.1 M KCl correlate well with the increase in viscosity with ionic strength observed for 80DT but not for 40DT (Figure 3). Due to the higher degree of hydrophobic modification, the mean distance between dodecyl chains is smaller for 80DT than for 40DT. When unimolecular micelles are formed, the polyelectrolyte backbone is forced to bend. Due to packing constraints it is unlikely that all hydrophobic groups will be accommodated in the core volume of the unimolecular micelles, but rather some of them remain in contact with the aqueous phase. This assumption is supported by our viscosity and DLS data. Dodecyl chains remaining outside the core of the unimolecular micelles will, at a sufficiently high ionic strength, start to interact with each other, forming intermolecular aggregates. Taking into consideration the screening length values for the different ionic strengths, we can estimate when the hydrophobic (short-range) attractive interactions would overcome electrostatic (long-range) repulsive interactions. The distance between the center of the nitrogen atom and the end of the dodecyl chain is approximately 17 Å. When dodecyl chains from different polymer molecules approach each other and start to interact, the distance between the positive charges of the quaternary ammonium groups from different molecules reaches 2×17 Å $= 34$ Å or less. The positively charged polymer molecules can approach such a distance only if the Debye length κ^{-1} is about this value or lower. This condition is fulfilled in the 0.01 M KCl solution, where κ^{-1} is 30.4 Å. Indeed, we observed a minimum in the viscosity close to this salt concentration. In a 0.1 M KCl solution the Debye length is about 9.6 Å and the unfavorable electrostatic interactions are significantly screened at this distance; thus hydrophobic segments from neighboring molecules can freely associate with each other. This in turn leads to phase separation when either the polymer concentration or the ionic strength is increased.

5. Concluding Remarks

On the basis of results from the combination of different techniques employed in this study, we are able to present a model of bulk and interfacial behavior of 40DT and 80DT. This is schematically illustrated in Figure 12. 40DT forms unimolecular micelles (intramolecular aggregates) where essentially all dodecyl chains are packed into the hydrophobic core. The outer part of the polymeric micelle consists of hydrophilic cationic units. The 80DT also forms unimolecular aggregates; however, it contains twice as many hydrophobic side chains and it is not possible to pack all of the side chains inside the unimolecular micelle. Therefore, some of the dodecyl chains remain outside the hydrophobic core, which facilitates formation of larger aggregates in bulk solution when the 80DT concentration and the ionic strength are sufficiently high. No similar aggregates could be detected for 40DT.

There is clearly a delicate balance between the short-range attractive van der Waals, hydrophobic interactions and the long-range repulsive electrostatic one, a balance that can be tuned by environmental conditions, e.g., ionic strength.

The surface excess of both 40DT and 80DT at the silica–water interface is, at low ionic strength, relatively low with an essentially flat adsorbed conformation of the polyamphiphiles. Nevertheless, the charges brought to the surface by the adsorbing polymers strongly overcompensate the silica surface charge. The adsorption is limited by the electrostatic repulsion between segments within the adsorption layer.

As the ionic strength of the solution increases, an increase in the adsorbed amount and a more extended conformation of the polyamphiphile away from the surface are observed. When the ionic strength is high enough, 80DT starts to form weakly adsorbed multilayers at the interface. The formation of the multilayers is controlled by the interaction between the dodecyl chains already located at the interface and the dodecyl segments present outside the core of the unimolecular micelles.

Acknowledgment. This work was financed by a grant from the Swedish Foundation for Strategic Research (Stiftelsen för Strategisk Forskning, SSF), through its Program for Surface and Colloid Technology (COLINTECH). The silica slides were kindly provided by Dr. Stefan Welin-Klintsröm, Linköping University. Emma Sparr is gratefully acknowleged for the help with atomic force microscopy.

LA047311Y